Journal of Statistical Physics, Vol. 63, Nos. 5/6, 1991

A Stochastic Model of Three-Dimensional Crystal Growth

Claude Garrod[1]

Received February 15, 1991

This paper describes a stochastic model of crystallization from a gas or dilute solution. The model is limited to a crystal of rectangular symmetry whose surface has nonzero Miller indices. By a mapping into the modified KDP model, the kinetic growth coefficient can be given approximately as an analytic function of the Miller indices of the surface. Numerical simulations indicate that the aproximation is accurate within a few percent at all surface orientations.

KEY WORDS: Crystal growth; six-vertex model.

1. INTRODUCTION

The study of crystal growth, from a macroscopic point of view, requires two basic parameters, the surface tension and the kinetic growth coefficient. Both parameters depend, in general, upon temperature, pressure (to a lesser extent), and the orientation of the crystal surface with respect to the fundamental crystal planes. One of the objects of microscopic studies of crystal growth is the calculation of those two parameters from a reasonable microscopic model of the crystal growth process. The surface tension, being an equilibrium property, has received the most detailed and successful study. In this paper, I will focus on the orientation dependence of the kinetic growth coefficient, to be defined below.

2. DEFINITION OF THE MODEL

We consider a crystal of simple cubic symmetry. (The generalization of the analysis to the case of rectangular symmetry is completely trivial.) If we

[1] Department of Physics, University of California, Davis, California 95616-8677.

0022-4715/91/0600-0987$06.50/0

cut the crystal with a plane that does not contain any primitive lattice vector, remove all particles above the plane, and assume that no surface reconstruction takes place, then we are left with a crystal surface of the general structure shown in Fig. 1. We replace the discarded portion by a gas with which the crystal continuously exchanges particles. In the configuration shown in Fig. 1 the most energetically favorable vacant sites are clearly the inside corners with three nearest neighbors. We call them condensation sites and assume that any particle condensing onto the surface either condenses directly into a condensation site or rapidly makes its way to one. Thus the crystal adds particles only at condensation sites. We assume that the condensation events at different sites are statistically independent and that the probability of a site being filled during time interval dt is $C\,dt$, where C is proportional to the flux of particles from the gas, the proportionality constant being some function of the temperature. Since the flux is proportional to the gas pressure we can write C in terms of the pressure as

$$C = \psi(T)P \tag{1}$$

The most weakly bound of the occupied sites are outside corner sites with three nearest neighbors. We call these evaporation sites and assume that particles are lost only from evaporation sites at a rate of E per site, where E is a function of temperature only,

$$E = \phi(T) \tag{2}$$

The detailed solution of the problem will verify the unsurprising fact that the condition for equilibrium is that $C = E$. At equilibrium the gas

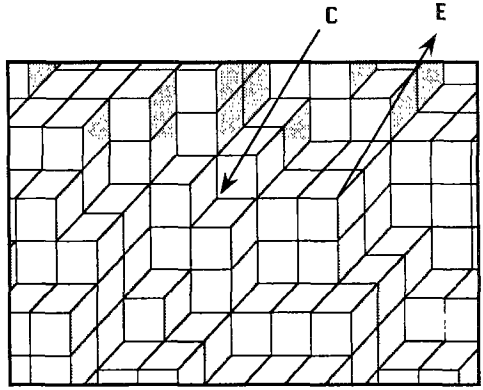

Fig. 1. The model of the crystal surface used in this paper. It is commonly referred to as the terrace-ledge-kink model. Inside corner sites are condensation sites and outside corner sites are evaporation sites.

pressure must be equal to the two-phase equilibrium pressure $P^e(T)$. This gives a relation between ψ and ϕ,

$$\phi(T) = \psi(T)\, P^e(T) \tag{3}$$

Away from equilibrium, the growth rate G, defined below, is given by

$$G = N_C \psi P - N_E \psi P^e \tag{4}$$

where G is the net rate at which particles are added to the crystal per unit area and N_C and N_E are the average numbers of condensation and evaporation sites per unit area, all areas being measured on the surface of the crystal. For small values of $\Delta P = P - P^e$ we can expand Eq. (4) to first order in ΔP, using the fact that $N_C = N_E$ at equilibrium:

$$G = \psi N_C^e \, \Delta P + \psi P^e \frac{\partial (N_C - N_E)}{\partial P} \Delta P \tag{5}$$

In Section 8 we shall show, by means of numerical simulations, that the second term on the right is never more than 4% of the first term for any orientation of the surface. If we drop that term and use the thermodynamic relation $(\partial P/\partial \mu)_T = 1/v(P, T)$, v being the volume per particle in the gas, we obtain

$$G = \frac{\psi}{v^e} N_C^e \, \Delta \mu \tag{6}$$

where, of course, $\Delta \mu$ is the difference between the actual chemical potential of the gas and the equilibrium value of μ at temperature T.

The kinetic growth coefficient K, defined as the ratio of G to $\Delta \mu$, is then given by

$$K = \frac{\psi}{v^e} N_C^e \tag{7}$$

We have no way of determining the function $\psi(T)$. Our aim in this paper is to compute N_C^e, which is a function of the surface orientation. We shall then have related the kinetic coefficient at one surface orientation to that at any other at the same temperature. This means that, if we watch an initially cubic sample dissolve, the sequence of shapes it passes through are predictable by this theory, but the rate at which it evolves from one shape to another, being dependent on the function $\psi(T)$, is not.

3. MAPPING TO A SIX-VERTEX MODEL

For convenience, we shall take the lattice spacing as our unit of length. A contour plot of the crystal surface, obtained by drawing a path in the x–y plane along the ledge at each height $z = n$, gives a series of paths that go either to the right or up and that may coincide (indicating a ledge of height greater than one), but never cross. The no-crossing rule is a consequence of the fact that the assumptions of the model prevent the creation of overhangs. An example is shown in Fig. 2. The orientation of the surface is determined by the average linear densities of paths cutting the x and y axes, which we call D_x and D_y, respectively. In interpreting the diagram we assume that the elevation of the surface increases in the negative x and positive y directions. Then the orientation of the surface is given by $\partial z/\partial x = -D_x$ and $\partial z/\partial y = D_y$.

To map the set of diagrams allowed by the "no-crossing" rule into the diagrams of a six-vertex model we make the following transformation. We number the paths with an integer K, equal to the z coordinate of the ledge. We then move the Kth path K units up and K units to the left. With this transformation the "no-crossing" diagrams are mapped one-to-one into the set of diagrams that satisfy a "no-touching" rule. The densities of path crossing the x and y axes in the new representation are d_x and d_y, where

$$d_x = D_x/(1 + D_x + D_y), \qquad d_y = D_y/(1 + D_x + D_y) \tag{8}$$

The inverse transformation, which we will need later, is

$$D_x = d_x/(1 - d_x - d_y), \qquad D_y = d_y/(1 - d_x - d_y) \tag{9}$$

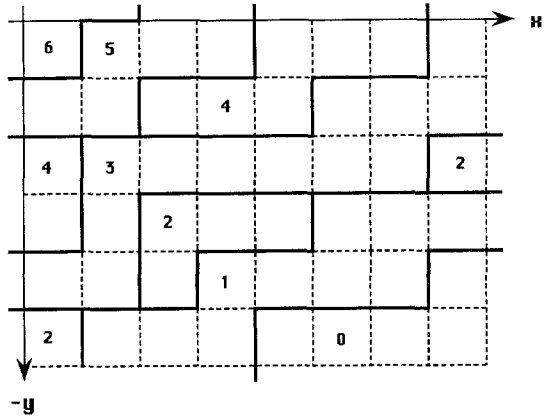

Fig. 2. A view of the crystal surface along the z axis. The numbers give the z coordinates of the "terraces."

It is convenient to calculate at this point, for subsequent use, how surface areas transform under this transformation. In Fig. 3a a section of the crystal surface is shown that intersects the x, y, and z axes at points a, $-b$, and c, respectively. The area of that piece of surface is $S_0 = \frac{1}{2}(a^2b^2 + a^2c^2 + b^2c^2)^{1/2}$. After the transformation, that area is transformed into the triangle shown in Fig. 3b, which has area $S_1 = \frac{1}{2}(ab + ac + bc)$. In terms of the Miller indices of the surface[2] $(k, l, m) \equiv (bc, ac, ab)$ we get $S_1/S_0 = (k + l + m)/(k^2 + l^2 + m^2)^{1/2}$. What is noteworthy is that the transformed area is clearly independent of which axis is chosen as the z axis in

[2] Actually, $(k, -l, m)$ are the Miller indices of the surface, as they are usually defined.

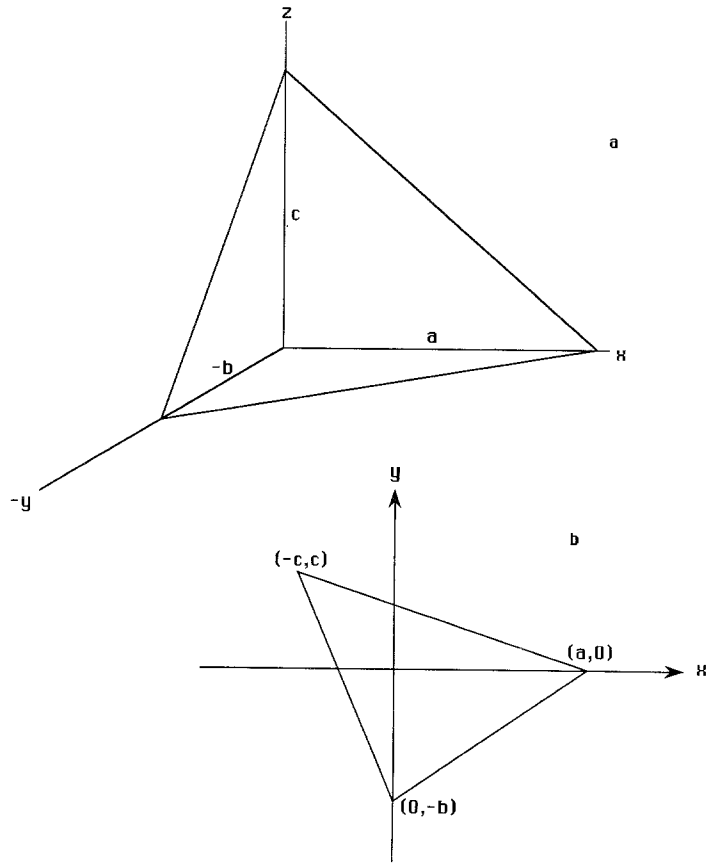

Fig. 3. (a) A portion of the crystal surface in three dimensions. (b) The projection of that portion on the x–y plane after the transformation described in the text.

making the transformation, even though, once an axis is chosen, the geometry of the transformation is quite unsymmetrical.

In order to avoid edge effects, we shall consider an infinite system with uniform macroscopic orientation. However, to make the model more precise, the infinite system will be obtained as the limit of a finite system with periodic boundary conditions. We therefore consider an $N \times N$ lattice with a number of paths drawn on it that go only up or to the right. If a path exits the lattice on the right, then one enters at a corresponding position on the left and the same is true with respect to the top and bottom. A possible configuration of a 5×5 lattice is shown in Fig. 4a. The five possible vertex configurations are shown in Fig. 4b. The numbering conforms with the usual numbering of the vertices in the well-known six-vertex model.[1] The allowed configurations in our "five-vertex" model are equivalent (by an exchange between blank and filled lines) to the allowed configurations of a particular six-vertex model, the modified KDP model, introduced by Wu.[2] This maping to the modified KDP model has previously been used by Blöte and Hilhorst to study the equilibrium properties of the crystal surface model used here.[3]

4. STEADY-STATE PROPERTIES

Before launching into the mathematical details of the solution of the model, we want to establish certain general properties of the model's dynamics. We define a $\binom{6}{1}$ plaquette as any square with a six-vertex in the upper left-hand corner and a one-vertex in the lower right-hand corner. A $\binom{1}{5}$ plaquette is defined in an obvious corresponding way. On our periodic

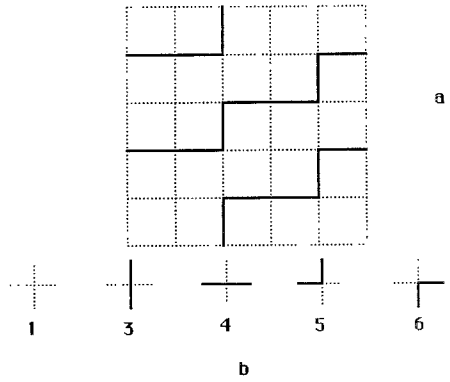

Fig. 4. (a) A possible configuration of the transformed lattice. (b) The numering of the five allowed vertices.

$N \times N$ lattice there is a stochastic process operating that randomly converts $(^6_1)$ plaquettes to $(^1_5)$ plaquettes at a rate C and makes the inverse transformation at a rate E. If we let N_x be the number of paths cutting any horizontal line through the lattice and N_y be the same thing for a vertical line, then N_x and N_y are obviously conserved by the stochastic process. We can thus consider separately sets of configurations that have fixed values for N_x and N_y. It is also obvious that the values of d_x and d_y are fixed in the thermodynamic limit by having $N_x/N \to d_x$, and $N_y/N \to d_y$. From now on, an "allowed" configuration implies definite values of N_x and N_y. The following theorem establishes the steady-state ensemble for a finite lattice under the equilibrium condition, $C = E$.

Theorem. For $C = E$ the steady-state ensemble assigns equal probability to every allowed configuration.

Proof. Let us denote the allowed configurations by letters $a, b, \ldots$, $P(a, t)$ is the probability of finding the system in state a at time t; $P(a, t)$ will satisfy a master equation of the form

$$\dot{P}(a) = -P(a) \sum_{b \neq a} T(a \to b) + \sum_{b \neq a} P(b)\, T(b \to a)$$

$$\equiv \sum_b T(a \mid b)\, P(b) \tag{10}$$

For fixed a, $T(b \to a)$ will be C (or E) if configurations b and a differ by a single condensation (or evaporation) event. Thus, if $T(b \to a) = C$, then $T(a \to b) = E$. This means that the diagonal element $T(a \mid a)$ is equal to the negative of the sum over b of the off-diagonal elements $T(a \mid b)$ with C and E interchanged. If $C = E$, then the sum of the elements in each row of $T(a \mid b)$ is zero. The condition for a steady-state solution is that $P(a)$ be a null vector of $T(a \mid b)$. Obviously, a vector with equal coefficients is a null vector of a matrix whose rows all have zero sum.

5. TRANSFORMATION TO A DIMER PROBLEM

Our aim is to calculate the density of $(^6_1)$ plaquettes as a function of the parameters d_x and d_y. Because of the symmetry exploited in the proof of the theorem, the density of $(^1_5)$ plaquettes is equal to the density of $(^6_1)$ plaquettes at equilibrium. The density of $(^6_1)$ plaquettes is an element of the two-point density function for next-nearest neighbors. We shall calculate it by making a transformation, introduced by F. Y. Wu, to a somewhat simpler dimer problem on a hexagonal lattice. In Fig. 5 a hexagonal dimer lattice is superimposed on the square lattice of our model. The rules that

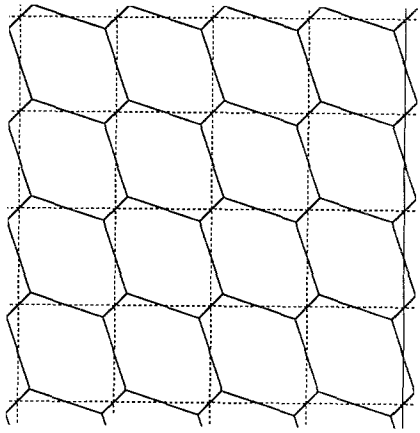

Fig. 5. The superposition of a hexagonal dimer lattice onto the square lattice.

define the allowed configuations of a dimer lattice are that every *link* (line between two nearest neighbor vertices) may be occupied by a *dimer* (indicated by heavy line) or it may be unoccupied. Every vertex must be the terminal point of exactly one dimer. If we identify the nearly vertical (or horizontal) dimers on the hexagonal lattice with vertical (or horizontal) paths on the square lattice, it is easy to see that the allowed dimer configurations are mapped one-to-one into the allowed path configurations on the square lattice. We index the plaquettes and the corresponding hexagons by two integers (x, y), which are just the coordinates of their upper left-hand corners. If the plaquette (x, y) is a condensation site, then the dimer configuration of the corresponding hexagon is as shown in Fig. 6. The density of such dimer configurations is a certain three-point correlation function on the dimer lattice which we can calculate as follows.

6. GENERAL FORMULAS FOR THE CORRELATION FUNCTIONS

We number the links of a finite dimer lattice, in an arbitrary way, from 1 to K. To the ith link we assign an energy v_i and an occupation number N_i, which can take the values 0 or 1. The allowed configurations of the lattice are denoted by the symbol C. The energy of configuration C is a sum of the energies of the occupied links

$$E(C) = \sum_{i=1}^{K} N_i(C) v_i \tag{11}$$

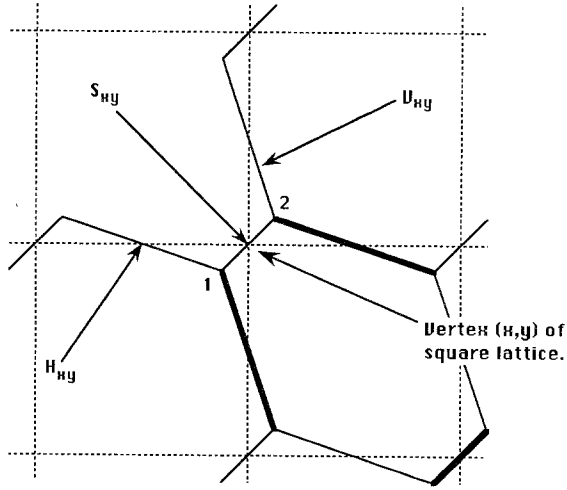

Fig. 6. The naming of the Boltzmann weights and the vertices on the hexagonal dimer lattice.

The partition function is given by

$$Z = \sum_C \exp\left(-\sum_i N_i v_i\right) \tag{12}$$

The probability of configuration C is assumed to be

$$P(C) = \exp[-E(C)]/Z \tag{13}$$

The one-, two-, and three-point distribution functions are defined by

$$F(i) = \sum_C N_i(C)\, P(C) = \sum_C N_i \left[\exp\left(-\sum N_j v_j\right)\right] \Big/ Z \tag{14}$$

$$F(i, j) = \sum_C N_i N_j P(C) = \sum_C N_i N_j \left[\exp\left(-\sum N_k v_k\right)\right] \Big/ Z \tag{15}$$

and

$$F(i, j, k) = \sum_C N_i N_j N_k P(C) = \sum_C N_i N_j N_k \left[\exp\left(-\sum N_l v_l\right)\right] \Big/ Z \tag{16}$$

$F(i, j, k)$ is the probability that links i, j, and k are simultaneously occupied. If we define the potential $\Omega = \log Z$, then

$$F(i) = -\frac{\partial \Omega}{\partial v_i} \tag{17}$$

$$F(i, j) = \frac{\partial^2 \Omega}{\partial v_i\, \partial v_j} + F(i)\, F(j) \tag{18}$$

and

$$F(i, j, k) = -\frac{\partial^3 \Omega}{\partial v_i \, \partial v_j \, \partial v_k} + F(i, j) F(k) + F(i, k) F(j) + F(j, k) F(i) - 2F(i) F(j) F(k) \tag{19}$$

7. THE BOLTZMANN WEIGHTS

If, for the horizontal, slanted, and vertical dimers at square vertex (x, y), we assign the Boltzmann weights $H_{xy} = \exp(-h_{xy})$, $S_{xy} = \exp(-s_{xy})$, and $V_{xy} = \exp(-v_{xy})$, respectively, then the partition function is equal to the square root of the determinant of the $2N^2$ by $2N^2$ matrix $M(x, y, \sigma \mid x', y', \sigma')$, where x, y, x', y' go from 0 to N and σ, σ' go from 1 to 2. The value 0 is identified with the value N in order to make the system periodic in x and y. The matrix elements of $M(x, y, \sigma \mid x', y', \sigma')$ are given by the formulas (see Fig. 6)

$$M(x, y, 1 \mid x, y, 2) = -M(x, y, 2 \mid x, y, 1) = S_{xy} \tag{20}$$

$$M(x-1, y, 2 \mid x, y, 1) = -M(x, y, 1 \mid x-1, y, 2) = H_{xy} \tag{21}$$

$$M(x, y, 2 \mid x, y+1, 1) = -M(x, y+1, 1 \mid x, y, 2) = V_{xy} \tag{22}$$

For the "unperturbed" case S, H, and V are constants (independent of x and y). In order to evaluate the distribution functions we shall have to perturb some of them infinitesimally. The unperturbed matrix we call M_0. Then

$$\Omega = \tfrac{1}{2} \log(\det M) = \tfrac{1}{2} \operatorname{tr}(\log M) \tag{23}$$

We let

$$M = M_0 + A = M_0 + A_1 + A_2 + A_3 \tag{24}$$

where the nonzero elements of A_1, A_2, and A_3 are

$$A_1(1, 0, 1 \mid 1, 0, 2) = -A_1(1, 0, 2 \mid 1, 0, 1) \equiv \varepsilon_1 = \delta S_{10} \tag{25}$$

$$A_2(0, 0, 2 \mid 0, 1, 1) = -A_2(0, 1, 1 \mid 0, 0, 2) \equiv \varepsilon_2 = \delta V_{00} \tag{26}$$

$$A_3(0, 1, 2 \mid 1, 1, 1) = -A_2(1, 1, 1 \mid 0, 1, 2) \equiv \varepsilon_3 = \delta H_{11} \tag{27}$$

These perturbations will allow us to calculate the probability of getting a condensation site at $(x, y) = (0, 1)$. We calculate the perturbed potential as follows:

$$M = M_0 + A = M_0(1 + B), \qquad \text{where} \quad B = M_0^{-1} A \tag{28}$$

Thus,

$$\Omega = \tfrac{1}{2}\operatorname{tr}(\log M) = \Omega_0 + \tfrac{1}{2}\operatorname{tr}[\log(1+B)] \tag{29}$$

We can use the expansion

$$\log(1+B) = B - \tfrac{1}{2}B^2 + \tfrac{1}{3}B^3 + \cdots \tag{30}$$

to obtain Ω as a power series in ε_1, ε_2, and ε_3.

We transform all matrices to a "momentum representation" by

$$M(k, l, \sigma \mid k', l', \sigma') = \frac{1}{N^2} \sum_{x, y, x', y'} e^{-i(kx+ly)} M(x, y, \sigma \mid x', y', \sigma') e^{i(k'x'+l'y')} \tag{31}$$

where k, l, k', and l' take the values $2\pi K/N$ with $K = 0, \ldots, N-1$. In the k, l representation

$$M_0(k, l, \sigma \mid k', l', \sigma') = \delta_{kk'}\delta_{ll'} m_{kl}(\sigma \mid \sigma') \tag{32}$$

with

$$m_{kl} = \begin{bmatrix} 0 & S - Ve^{-il} - H^{-ik} \\ -S + Ve^{il} + He^{ik} & 0 \end{bmatrix} \equiv \begin{bmatrix} 0 & \mu_{kl} \\ -\mu_{kl}^* & 0 \end{bmatrix} \tag{33}$$

In this representation $M_0^{-1} = \delta_{kk'}\delta_{ll'} m_{kl}^{-1}(\sigma \mid \sigma')$, where

$$m_{kl}^{-1} = \begin{bmatrix} 0 & -1/\mu_{kl}^* \\ 1/\mu_{kl} & 0 \end{bmatrix} \equiv \begin{bmatrix} 0 & -\gamma_{kl}^* \\ \gamma_{kl} & 0 \end{bmatrix} \tag{34}$$

and A_1, A_2, and A_3 have the forms

$$A_1(k, l, \sigma \mid k', l', \sigma') = \varepsilon_1 N^{-2} e^{i(k'-k)}(\delta_{\sigma,1}\delta_{\sigma',2} - \delta_{\sigma,2}\delta_{\sigma',1}) \tag{35}$$

$$A_2(k, l, \sigma \mid k', l', \sigma') = \varepsilon_2 N^{-2}(e^{il'}\delta_{\sigma,2}\delta_{\sigma',1} - e^{-il}\delta_{\sigma,1}\delta_{\sigma',2}) \tag{36}$$

and

$$A_3(k, l, \sigma \mid k', l', \sigma') = \varepsilon_3 N^{-2}(e^{i(k'+l'-l)}\delta_{\sigma,2}\delta_{\sigma',1} - e^{-i(k+l-l')}\delta_{\sigma,1}\delta_{\sigma',2} \tag{37}$$

Multiplying A_1, A_2, and A_3 by M_0^{-1}, we get

$$B_1 = \varepsilon_1 N^{-2} e^{i(k'-k)}(\gamma_{kl}^*\delta_{\sigma,1}\delta_{\sigma',1} + \gamma_{kl}\delta_{\sigma,2}\delta_{\sigma',2}) \tag{38}$$

$$B_2 = -\varepsilon_2 N^{-2}(\gamma_{kl}^* e^{il'}\delta_{\sigma,1}\delta_{\sigma',1} + \gamma_{kl} e^{-il}\delta_{\sigma,2}\delta_{\sigma',2}) \tag{39}$$

and

$$B_3 = -\varepsilon_3 N^{-2}(\gamma_{kl}^* e^{i(k'+l'-l)}\delta_{\sigma,1}\delta_{\sigma',1} + \gamma_{kl} e^{-i(k+l-l')}\delta_{\sigma,2}\delta_{\sigma',2}) \tag{40}$$

We now have to calculate the product matrices $B_1 \cdot B_2 \equiv B_{12}$, $B_1 \cdot B_2 \cdot B_3 \equiv B_{123}$, etc. Before we do so we define certain functions that will appear in the calculations:

$$f_1(a, b, c) = \int_0^{2\pi} dk \int_0^{2\pi} dl \frac{1}{a - be^{il} - ce^{ik}} \tag{41}$$

$$f_2(a, b, c) = \int_0^{2\pi} dk \int_0^{2\pi} dl \frac{e^{ik}}{a - be^{il} - ce^{ik}} \tag{42}$$

$$f_3(a, b, c) = \int_0^{2\pi} dk \int_0^{2\pi} dl \frac{e^{i(l-k)}}{a - be^{il} - ce^{ik}} \tag{43}$$

With these definitions we get

$$B_{12}(k, l, \sigma | k', l', \sigma') = -\frac{\varepsilon_1 \varepsilon_2}{4\pi^2 N^2} [f_2(S, V, H)\, e^{i(l'-k)} \gamma_{kl}^* \delta_{\sigma,1} \delta_{\sigma',1} + f_3(S, V, H)\, e^{-ik} \gamma_{kl} \delta_{\sigma,2} \delta_{\sigma',2}] \tag{44}$$

$$B_{21} = -\frac{\varepsilon_1 \varepsilon_2}{4\pi^2 N^2} [f_3(S, V, H)\, e^{ik'} \gamma_{kl}^* \delta_{\sigma,1} \delta_{\sigma',1} + f_2(S, V, H) e^{i(k'-l)} \gamma_{kl} \delta_{\sigma,2} \delta_{\sigma',2}] \tag{45}$$

$$B_{13} = -\frac{\varepsilon_1 \varepsilon_3}{4\pi^2 N^2} [f_3(S, V, H) e^{i(k'+l'-k)} \gamma_{kl}^* \delta_{\sigma,1} \delta_{\sigma',1} + f_2(S, H, V) e^{i(l'-k)} \gamma_{kl} \delta_{\sigma,2} \delta_{\sigma',2}] \tag{46}$$

$$B_{31} = -\frac{\varepsilon_1 \varepsilon_3}{4\pi^2 N^2} [f_2(S, H, V) e^{i(k'-l)} \gamma_{kl}^* \delta_{\sigma,1} \delta_{\sigma',1} + f_3(S, V, H) e^{i(k'-k-l)} \gamma_{kl} \delta_{\sigma,2} \delta_{\sigma',2}] \tag{47}$$

$$B_{23} = \frac{\varepsilon_2 \varepsilon_3}{4\pi^2 N^2} [f_1(S, V, H) e^{i(k'+l')} \gamma_{kl}^* \delta_{\sigma,1} \delta_{\sigma',1} + f_3(S, V, H) e^{i(l'-l)} \gamma_{kl} \delta_{\sigma,2} \delta_{\sigma',2}] \tag{48}$$

$$B_{32} = \frac{\varepsilon_2 \varepsilon_3}{4\pi^2 N^2} [f_3(S, V, H) e^{i(l'-l)} \gamma_{kl}^* \delta_{\sigma,1} \delta_{\sigma',1} + f_1(S, V, H) e^{i(k+l)} \gamma_{kl} \delta_{\sigma,2} \delta_{\sigma',2}] \tag{49}$$

$$B_{123} = \frac{\varepsilon_1 \varepsilon_2 \varepsilon_3}{16\pi^4 N^2} [f_1(S, V, H)\, f_2(S, V, H) e^{i(k'+l'-k)} \gamma_{kl}^* \delta_{\sigma,1} \delta_{\sigma',1} + f_3(S, V, H)\, f_3(S, V, H) e^{i(l'-k)} \gamma_{kl} \delta_{\sigma,2} \delta_{\sigma',2}] \tag{50}$$

and

$$B_{132}=\frac{\varepsilon_1\varepsilon_2\varepsilon_3}{16\pi^4N^2}\left[f_3(S,V,H)f_3(S,V,H)e^{i(l'-k)}\gamma^*_{kl}\delta_{\sigma,1}\delta_{\sigma',1}\right.$$
$$\left.+f_1(S,V,H)f_2(S,H,V)e^{-ik}\gamma_{kl}\delta_{\sigma,2}\delta_{\sigma',2}\right] \tag{51}$$

The integrals defining f_1, f_2, and f_3 can be evaluated by standard contour integration techniques. If we assume that a, b, and c form a triangle (a condition that will be true within our physical parameter space), then

$$f_1(a,b,v)=\frac{4\pi}{a}\theta_a \tag{52}$$

$$f_2(a,b,c)=-\frac{4\pi}{c}\theta_c \tag{53}$$

and

$$f_3(a,b,c)=-\frac{4\pi}{a}\sin\theta_a \tag{54}$$

where θ_a, θ_b, and θ_c are the angles opposite the sides a, b, and c in the triangle with those sides. Note that, by the law of sines, f_3 is symmetric in a, b, and c.

We can now calculate all the traces needed in the power series expansion given by Eqs. (29) and (30). They are

$$\mathrm{tr}(B_1)=\frac{\varepsilon_1}{2\pi^2}f_1(S,V,H)=\frac{2\varepsilon_1\theta_S}{\pi S} \tag{55}$$

$$\mathrm{tr}(B_2)=-\frac{\varepsilon_2}{2\pi^2}f_2(S,H,V)=\frac{2\varepsilon_2\theta_V}{\pi V} \tag{56}$$

$$\mathrm{tr}(B_3)=-\frac{\varepsilon_3}{2\pi^2}f_2(S,V,H)=\frac{2\varepsilon_3\theta_H}{\pi H} \tag{57}$$

$$\mathrm{tr}(B_{12})=-\frac{\varepsilon_1\varepsilon_2}{8\pi^4}f_2(S,V,H)f_3(S,V,H)=-\frac{2\varepsilon_1\varepsilon_2\theta_H\sin\theta_V}{\pi^2HV} \tag{58}$$

$$\mathrm{tr}(B_{13})=-\frac{\varepsilon_1\varepsilon_3}{8\pi^4}f_2(S,H,V)f_3(S,V,H)=-\frac{2\varepsilon_1\varepsilon_3\theta_V\sin\theta_H}{\pi^2HV} \tag{59}$$

$$\mathrm{tr}(B_{23})=\frac{\varepsilon_2\varepsilon_3}{8\pi^4}f_1(S,V,H)f_3(S,V,H)=-\frac{2\varepsilon_2\varepsilon_3\theta_S\sin\theta_S}{\pi^2S^2} \tag{60}$$

$$\mathrm{tr}(B_{123})=\frac{\varepsilon_1\varepsilon_2\varepsilon_3}{64\pi^6}\left[f_1(S,V,H)f_2(S,V,H)f_2(S,H,V)+f_3^3(S,V,H)\right]$$
$$=\frac{\varepsilon_1\varepsilon_2\varepsilon_3}{\pi^3}\frac{\theta_S\theta_V\theta_H-\sin\theta_S\sin\theta_V\sin\theta_H}{SVH}=\mathrm{tr}(B_{132}) \tag{61}$$

We now have all the machinery necessary to calculate the derivatives of Ω, which, by Eqs. (17)–(19), will yield the needed distribution functions. The one-point distributions, for slanted, vertical, and horizontal dimers, respectively, are

$$F(s) = -\frac{\partial \Omega}{\partial s_{10}} = S \left.\frac{\partial \Omega}{\partial \varepsilon_1}\right|_{\varepsilon = 0} = \frac{\theta_S}{\pi} \tag{62}$$

$$F(v) = V \left.\frac{\partial \Omega}{\partial \varepsilon_2}\right|_{\varepsilon = 0} = \frac{\theta_V}{\pi} \tag{63}$$

and

$$F(h) = H \left.\frac{\partial \Omega}{\partial \varepsilon_3}\right|_{\varepsilon = 0} = \frac{\theta_H}{\pi} \tag{64}$$

In the expressions $F(s)$, $F(v)$, and $F(h)$, the symbols s, v, and h are being used to indicate the slanted, vertical, and horizontal links, not the energy values on those links.

The other important distribution function is the threepoint distribution function, $F(s, v, h)$. After some algebra, we obtain

$$F(s, v, h) = \pi^{-3} \left(\frac{S}{H} \sin \theta_V \theta_H^2 + \frac{H}{V} \sin \theta_S \theta_V^2 + \frac{V}{S} \sin \theta_H \theta_S^2 \right.$$
$$\left. - \sin \theta_S \sin \theta_V \sin \theta_H + 2\theta_S \theta_V \theta_H \right) \tag{65}$$

This gives the probability that a given plaquette is a condensation site. It can be expressed as a function of the Miller indices of the surface as follows. If we draw a line in the x direction that lies between two rows of vertices, then the density of paths cutting that line is equal to $F(v)$. Thus, $d_x = F(v) = \theta_V/\pi$ and, in a similar way, $d_y = F(h) = \theta_H/\pi$. From Eq. (8) and Fig. 3a we can derive the following relations between d_x and d_y and the Miller indices (k, l, m):

$$d_x = \frac{k}{k+l+m} \qquad \text{and} \qquad d_y = \frac{l}{k+l+m}$$

From these it follows that

$$\theta_V = \frac{k\pi}{k+l+m} \tag{66a}$$

$$\theta_H = \frac{l\pi}{k+l+m} \tag{66b}$$

$$\theta_S = \frac{m\pi}{k+l+m} \tag{66c}$$

These three equations allow us to eliminate the variables S, V, and H in favor of the Miller indices of the surface. Only the ratios of Miller indices have significance. Therefore, we are free to impose the restriction that $k+l+m=1$ and will do so henceforth. A three-dimensional graph of F as a function of D_x and D_y is given in Fig. 7.

Since we are using units in which the lattice constant is unity, $F(s, v, h)$ gives the density of condensation sites on the x–y plane. To compute the kinetic coefficient, by Eq. (7), we must transform to area on the crystal surface. The result is given by

$$K=\frac{\psi(T)}{v^e(T)}\frac{F(s, v, h)}{(k^2+l^2+m^2)^{1/2}} \tag{67}$$

One sidelight of this analysis is that it, in a sense, explains a peculiar symmetry of the modified KdP model. Because of the sixfold rotational symmetry of the hexagonal lattice it is clear that the partition function is invariant with respect to permutations of the variables S, V, and H. A threefold symmetry is somewhat unnatural for a two-dimensional square lattice model. It is easy to see that this symmetry simply reflects the natural invariance of the condensation site density N_C with respect to permutation of the coordinate axes x, y, and z.

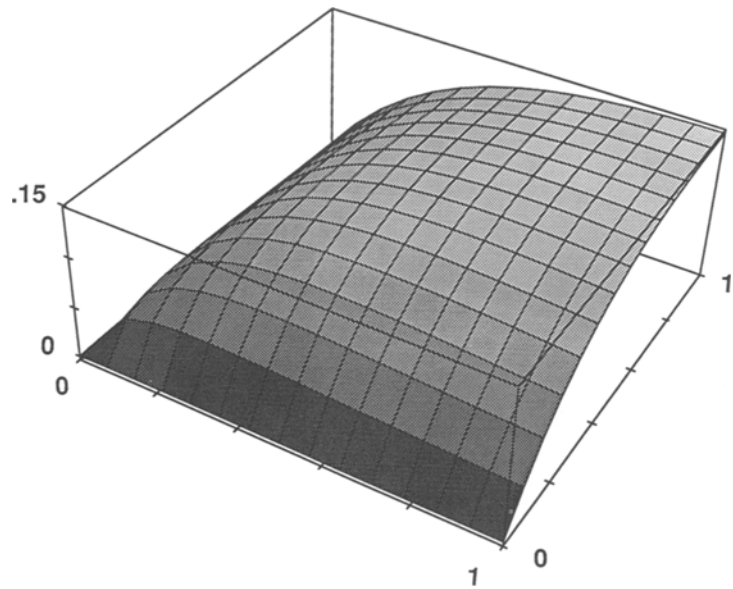

Fig. 7. The function $F(s, v, h)$, which gives the fraction of plaquettes that are condensation sites, as a function of D_x and D_y.

8. NUMERICAL SIMULATION

In this calculation we have neglected the second of the two terms in Eq. (5) for the growth rate as a function of the pressure imbalance. In order to determine the relative size of the neglected term I have performed numerical simulations of the crystal growth for finite lattices at various orientations and various values of C and E. Using Eqs. (1)–(3), we can rewrite Eq. (5) in the form

$$G = \psi \left(N_C^e + \frac{\partial (N_C - N_E)}{\partial \varepsilon} \right) \Delta P \tag{68}$$

where $\varepsilon = (C - E)/E$. The value of N_C^e is known, as a function of orientation, from the exact solution. The second term can be easily ascertained by numerical simulation of nonequilibrium growth. First it may be noted that, for any orientation that is close to a principal plane, the ledges are widely separated and therefore a treatment of them as noninteracting ledges would be appropriate. But, for any isolated ledge, the number of condensation sites is exactly equal to the number of evaporation sites and the neglected term is therefore zero.

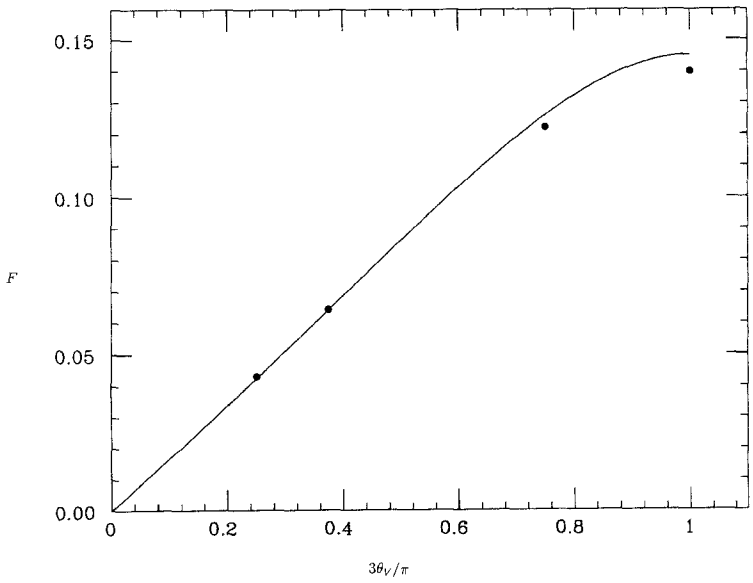

Fig. 8. A comparison of the analytic approximation with the results of numerical simulation. The curve gives $F(v, h, s)$ as a function of the ratio of θ_V to $\pi/3$ for the special case $\theta_V = \theta_H$. The points are the results of four numerical calculations.

The simulation of a stochastic process on a finite lattice is a straightforward matter. The correctness of the program and the errors due to finite-size effects and statistics can be determined by taking runs with $C = E$ and comparing the numerical results for $F(s, v, h)$ with Eq. (65). If the unknown functions $\psi(T)$ and $v_e(T)$ are taken to be unity, then Eq. (67) says that

$$F(s, v, h) = (k^2 + l^2 + m^2)^{1/2} K \tag{69}$$

In Fig. 8, a graph of F for the case $\theta_V = \theta_H$ is given as a function of θ_V for the range $0 < \theta_V < \pi/3$ and compared with four values of $(k^2 + l^2 + m^2)^{1/2} K$ obtained by simulating nonequilibrium growth. The size of the numerical data points gives an estimate of their accuracy. Their deviation from the analytic curve is due primarily to the neglected second term in Eq. (5). The error is always less than 4%.

ACKNOWLEDGMENTS

This article is dedicated to my former thesis advisor and longtime friend, Jerome K. Percus, on the occasion of his 65th birthday. I hope that this "96% solution" does not disfigure his commemerative volume. The author would like to thank A. C. Levi and E. Tosatti of SISSA, Trieste for valuable contributions to this work and Michael Brodheim of the Vacaville Medical Facility for a careful reading of the manuscript and the correction of a large number of minor errors.

REFERENCES

1. E. H. Lieb and F. Y. Wu, in *Phase Transitions and Critical Phenomena*, Vol. 1, C. Domb and M. S. Green, eds. (Academic Press, 1972).
2. F. Y. Wu, *Phys. Rev.* **168**:539 (1968).
3. H. W. J. Blöte and H. J. Hilhorst, *J. Phys. A* **15**:L631 (1982); see also B. Nienhuis, H. J. Hilhorst, and H. W. J. Blöte, *J. Phys. A* **17**:3359 (1984).